Electrochemical and Solid-State Letters, **14** (10) H422-H425 (2011)
1099-0062/2011/14(10)/H422/4/$28.00 © The Electrochemical Society

Realization of Rectifying and Resistive Switching Behaviors of TiO_2 Nanorod Arrays for Nonvolatile Memory

Feng Zhang,[a] Xiaoyan Gan,[a] Xiaomin Li,[a,z] Liang Wu,[a] Xiangdong Gao,[a] Renkui Zheng,[a] Yong He,[a] Xinjun Liu,[b] and Rui Yang[c]

[a]*State Key Laboratory of High Performance Ceramics and Superfine Microstructures, Shanghai Institute of Ceramics, Chinese Academy of Sciences, Shanghai 200050, People's Republic of China*
[b]*Department of Materials Science and Engineering, Gwangju Institute of Science and Technology, Buk-gu, Gwangju 500-712, Korea*
[c]*International Center for Materials Nanoarchitectonics, National Institute for Materials Science, Ibaraki 305-0044, Japan*

Both the rectifying and resistive switching behaviors are reported in single-crystalline TiO_2 nanorod arrays (NRAs). The transition from rectifying to bipolar resistive switching behavior can be controlled by a forming process. The surface of TiO_2 nanorods and the Pt/TiO_2 NRAs interface play crucial roles on resistive switching. In low resistance state, the dependence of resistance on cell area indicates that filaments form on each individual nanorod, which contributes to the narrow distribution of resistive switching parameters. These results suggest that single-crystalline TiO_2 NRAs could be used as nanowire-based switch element and memory cell for next-generation nonvolatile memory.
 [DOI: 10.1149/1.3617442]

Manuscript submitted April 15, 2011; revised manuscript received July 11, 2011. Published July 27, 2011.

Resistive switching random access memory (RRAM) based on resistive switching phenomenon has potential applications in next-generation nonvolatile memory,[1–4] and thus attracts extensive scientific and technological interests due to its high read/write speed and high data storage density.[1–3] Until now, the resistive switching phenomenon has been observed in various polycrystalline and amorphous thin films, including perovskite oxides,[4] NiO,[5] TiO_2,[6] ZnO,[7] and ZrO_2.[8] However, the underlying resistive switching mechanism is still not fully understood.[2] Moreover, the wide distribution of resistive switching parameters is believed to be one of most crucial obstacles for practical application of RRAM.[9] Recently, it was found that NiO,[10,11] CoO (Ref. 12) and ZnO (Refs. 13 and 14) nanowires and nanorods also display resistive switching behaviors. It is obvious that the study of nanowire-based RRAM is beneficial to obtain improved resistive switching characteristics and deepen our understanding of nanoscale resistive switching mechanisms.[9]

TiO_2 thin film is one of the best materials for use as RRAM (Ref. 9) and the fourth fundamental passive circuit arrays element (i.e., Memosistor).[15,16] It would be attractive that the realization of RRAM or even Memosistor on a single TiO_2 nanowire, so the study of TiO_2 nanowire-based memory cell is highly desired. Although many nanowire-based memory elements have been investigated, nanowire-based switch elements have yet not been reported for alleviating sneaking current in cross-bar array structures.[3,17,18] In this work, we demonstrate the rectifying and bipolar resistive switching behaviors in single-crystalline TiO_2 nanorod arrays (NRAs) and found that the transition from rectifying to bipolar resistive switching behavior is controlled by a forming process. Our results show that the single-crystalline TiO_2 NRAs has the potential for use as nanowire-based switch element or memory cell for next-generation nonvolatile memory.

Experimental

TiO_2 NRAs were grown on transparent fluorinated tin oxide (FTO) substrates (20 Ω/□) using a hydrothermal method.[19] Briefly, ultrasonically cleaned FTO substrates were placed up-side down in a sealed Teflon reactor (100 ml), containing 30 ml of deionized water, 30 ml of hydrochloric acid (37 wt %) and 0.8 ml of tetrabutyl titanate. The reactor was placed in an oven with a temperature of 180°C for 9 h. Then, the reactor was cooled rapidly to room temperature under flowing water. The substrates were taken out from the reactor, rinsed and dried. After the growth process, x-ray diffractometer (XRD, Cu Kα, RIGAKU, D/MAX-2550V), filed emissions scanning electron microscope (FESEM: S-4700, Hitachi) and JEM200CX transmission electron microscopy equipped with selected area electron diffraction (TEM/SAED) were employed to characterize the crystal structure and morphology of the TiO_2 NRAs. Pt top electrodes with a diameter of 100 μm were deposited by electron beam evaporation with a metal shadow mask. Current-voltage (*I-V*) characteristics were examined by a Keithley 2410c source meter unit by using a DC voltage sweeping. The bias voltage was applied to the Pt top electrode while the FTO bottom electrode was grounded during the electrical measurements.

Results and Discussion

A schematic configuration of the Pt/TiO_2 NRAs/FTO structure and a typical SEM image of TiO_2 NRAs are shown in Figs. 1a and 1b, respectively. It can be seen that the TiO_2 nanorods are vertically aligned on the FTO substrates. The average length and diameter of the nanorods are 2.5 μm and 130 nm, respectively. Figure 1c and the inset show a TEM image of a single TiO_2 nanorod and the corresponding SAED pattern of the nanorod, examined along the zone axis. The results indicate that the nanorods are single-crystal. From the XRD of the TiO_2 NRAs shown in Fig. 1d, the nanorods can be indentified as tetragonal rutile phase (JCPDS No.88-1175). The enhanced (002) peak indicates that the nanorods are well crystallized and grows preferentially perpendicular to the FTO substrate.

Figure 2 shows the initial current-voltage (*I-V*) characteristics of the Pt/TiO_2 NRAs/FTO structure. By sweeping bias voltage from -1.5 to $+1.5$ V, a clear rectifying behavior was observed. Since the work function of Pt (5.65 eV) is higher than the electron affinity of rutile TiO_2 (4.2 eV),[20] it is plausible that the Schottky behavior mainly originates from the Pt/TiO_2 NRAs junction. The inset in Fig. 2 shows that the forward/reverse current ratio (F/R ratio) and the forward current (1.5 V) are 10^4 and 3×10^{-4} A, respectively. In comparison with the desired value of thin-film switch element,[21,22] the F/R ratio and forward current of the Pt/TiO_2 NRAs/FTO diode are small. However, considering the small forward current of nanowire-based memory devices,[23] the relatively lower forward current and F/R ratio of Pt/TiO_2 NRAs/FTO switch element are large enough for nanowire-based memory devices. Therefore, the Pt/TiO_2 NRAs/FTO Socottky-type diode could be a promising switch element to alleviate sneaking current for nanowire-based memory device in cross-bar array structures. Nevertheless, it should be noted that Schottky-type diodes can only be used for unipolar resistive switching memory devices,[18] so the Pt/TiO_2 NRAs/FTO switch element cannot work for itself due to its bipolar resistive switching behavior.

[z] E-mail: lixm@mail.sic.ac.cn

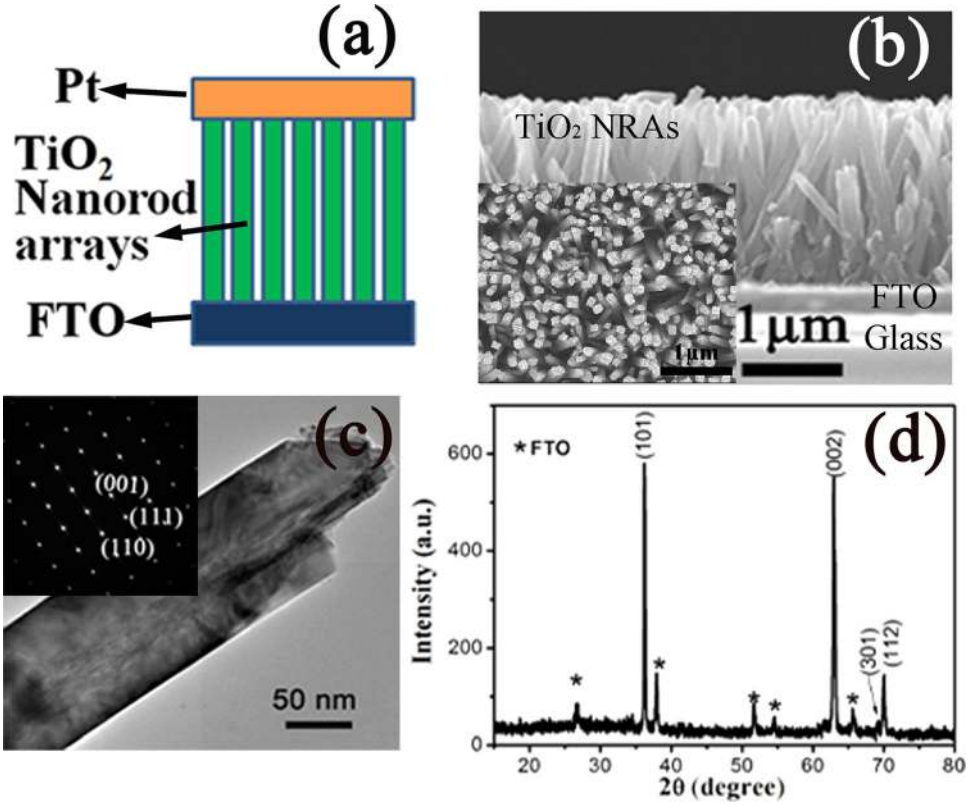

Figure 1. (Color online) (a) A schematic configuration of Pt/TiO_2 NRAs/FTO structure. (b) Cross-section SEM image, (c) TEM images and (d) XRD pattern of TiO_2 NRAs. The inset in (b) shows the top view SEM image of the TiO_2 nanorods. The inset in (c) shows the SAED pattern of the corresponding TiO_2 nanorod.

With a forming process, the rectifying behavior (see Fig. 2) was changed to bipolar resistive switching behavior, as shown in Fig. 3a. When the bias voltage is swept up to 6.7 V, the current increases dramatically to the current compliance of 20 mA. The large forming voltage could avoid the breakdown of the Pt/TiO_2 NRAs/FTO cell when it was used as switch element. For the forming process, when the bias voltage is lower than 4 V, the current increases gradually because of the increase in injected carriers with forward bias voltage on the Schottky type junction of Pt/TiO_2 NRAs. However, when the bias voltage is higher than 4 V, the current decreases slowly until the forming process occurs. We infer that the higher voltage propels the oxygen vacancies away from the Schottky type Pt/TiO_2 NRAs interface, causing a wider depletion layer and thus a decreasing current.[24] The initial resistance is 2×10^8 Ω, and the forming process switches the cell to a low resistance state (LRS) of approximately 130 Ω.

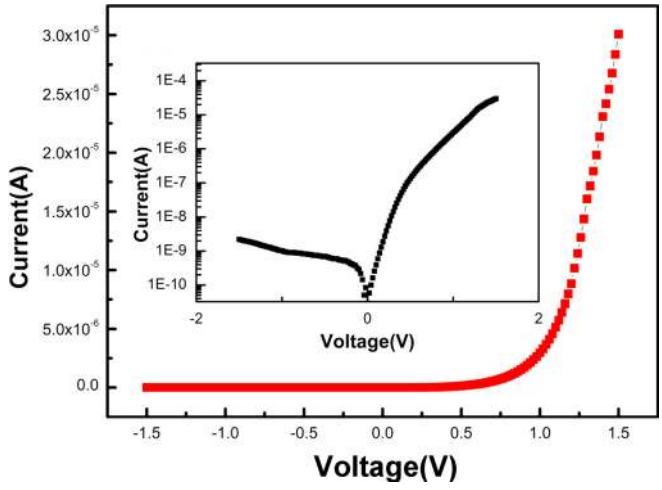

Figure 2. (Color online) Current-voltage (*I-V*) characteristics of the Pt/TiO_2 NRAs/FTO structure measured from −1.5 to 1.5 V. The inset shows the same *I-V* data in a semilogarithm scale.

After the forming process, the Pt/TiO_2 NRAs/FTO cell displays typical bipolar resistive switching behavior, as shown in Fig. 3b. The sweeping direction and the sequence are indicated by arrows and digits in the figure. When the bias voltage is swept from zero to negative values, the cell was switched to a high resistance state (HRS) at −1.5 V (reset voltage). The high resistance is about 1300 Ω. Accordingly, when the bias voltage is swept from zero to positive range, the cell was switched to LRS at +1.5 V (set voltage) with a current compliance of 20 mA. It is widely accepted that the resistive switching effects of thin films is due to the electric-field-induced drift of ion/defect through dislocations or grain boundaries.[2,24,25] Compared with that of TiO_2 thin films (tens of nanometers thick),[25] the TiO_2 NRAs with a length of 2.5 μm exhibit a lower field, but the forming and switching voltages almost remain unchanged. Since no grain boundaries are expected in single-crystalline TiO_2 NRAs, this phenomenon could be due to much higher mobility of defects on the surface of single-crystalline TiO_2 NRs.[13]

To further elucidate the switching and conducting mechanisms of the memory cell, the logarithmic plot and linear fitting of the forward and reverse voltage sweep region of the *I-V* characteristics are shown in Figs. 4a and 4b. A linear *I-V* curve with a slope of ~1 indicates an Ohmic conductive mechanism in LRS, indicating that the conducting filaments dominate the transport behavior.[26] However, a totally different transport mechanism was observed in HRS. The nonlinear region of the *I-V* curve at the high voltage in positive bias region can be well fitted by Schottky emission theory (linear dependence of $\ln(I/T^2)$ on $V^{1/2}$),[27] as shown in Fig. 4b. The Schottky interface dominated transport behavior in HRS suggests that Schottky-type Pt/TiO_2 NRAs junction is an important factor for resistive switching.

Based on the above results, the bipolar resistive switching mechanisms in the Pt/TiO_2 NRAs/FTO cell can be explained as follows. Under positive bias voltage, the oxygen vacancies drift toward cathode and accumulate at the cathode while oxygen ions migrate

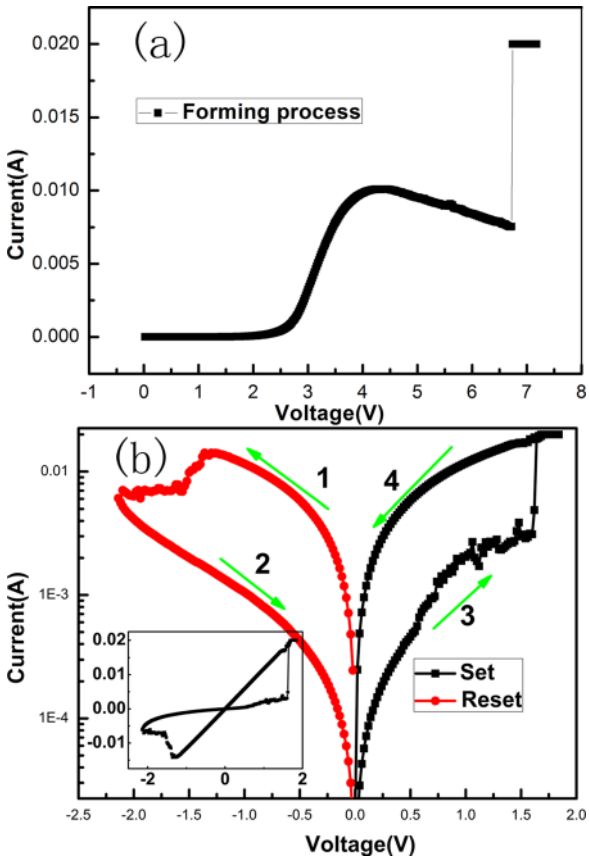

Figure 3. (Color online) (a) The forming process of the Pt/TiO_2 NRAs/FTO memory cell. (b) Typical bipolar resistance switching behaviors in a semilogarithm scale. The inset is the *I-V* characteristics in linearscale.

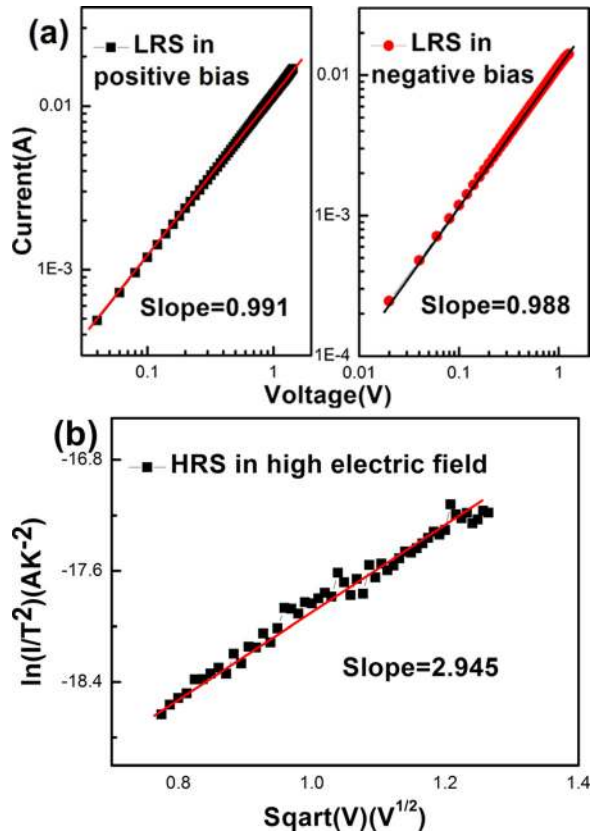

Figure 4. (Color online) (a) The forward and reverse bias of linear fitting of *I-V* curve in log-log scale for LRS. (b) The Schottky emission curve fitting for HRS in positive bias voltage region.

toward anode.[28,29] At a voltage of 6.7 V, the conducing filaments of oxygen vacancies penetrate the Schottky barrier and dominate the transport behavior. In the reset process with negative bias voltage, the filaments are ruptured by oxygen ion and the schottky interface controls the transport behavior. Accordingly, the residual filaments are recovered in the set process with positive bias voltage.

Large fluctuation of resistive switching parameters is thought to be a crucial obstacle for practical application of RRAM,[9] which is usually attributed to the random formation and rupture of conducting

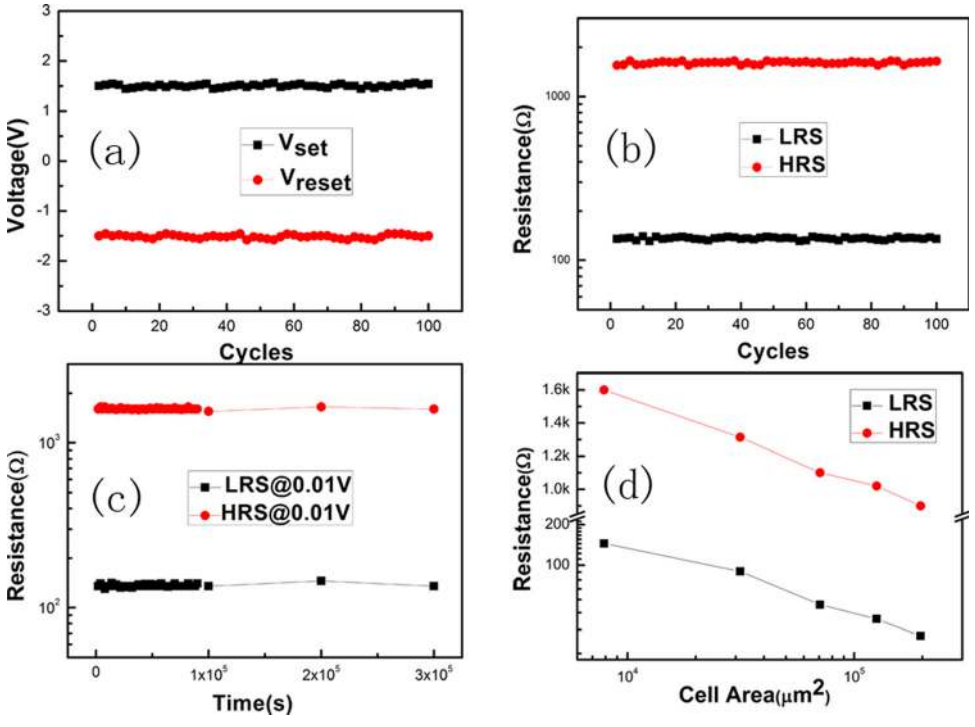

Figure 5. (Color online) Distribution of (a) switching voltages and (b) the high and low resistance state (HRS and LRS). (c) Retention of the Pt/TiO_2 NRAs/FTO memory cell. The resistance was read out at 0.01 V. (d) Cell area dependence of the LRS and HRS resistance, measured at a bias voltage of 0.02 V.

filaments.[30] The present Pt/TiO_2 NRAs/FTO memory cell displays narrow distributions of switching parameters (reset and set voltage, HRS and LRS) and long retention time, as shown in Figs. 5a–5c. In order to further understand the improved characteristic, the cell area dependence of resistance in HRS and LRS was investigated, as shown in Fig. 5d. Both the resistance in HRS and LRS decreases with increasing cell area. In contrast, for polycrystalline and amorphous thin films, the resistance in LRS usually show weakly dependent on cell area, which suggests that the resistive switching effects is closely related to localized filaments. For Pt/TiO_2 NRAs/FTO cell, the dependence of resistance in LRS on cell area does not mean filament model is not responsible for the resistance switching behavior. According to the above fitting results and the special structure of TiO_2 NRAs, we infer that each nanorod is conducted by individual filament. So the more nanorods covered by Pt electrode, the lower the resistance in LRS. These identical filaments may suppress the random formation of conducting filaments. More importantly, each filament is strictly confined within each nanorod, so the switching process could be easier to be controlled, giving rise to narrow dispersion of switching parameters.

Conclusions

In summary, both the rectifying and resistive switching characteristics were investigated in single-crystalline TiO_2 NRAs. The transition from rectifying to bipolar resistive switching behavior could be controlled by a forming process. Before the forming process, rectifying behavior was observed and it could be used as switch element for nanowire-based memory device to alleviate sneaking current in cross-bar array structures. After the forming process, The Pt/TiO_2 NRAs/FTO cell displays typical bipolar resistive switching behavior, a long retention time, and narrow distribution of the resistive switching parameters. These results demonstrate that single-crystalline TiO_2 NRAs have potential applications in RRAM.

Acknowledgments

The work was supported by Major Program of National Natural Science Foundation of China (Grant No. 90922026), Major State Basic Research Development Program(Grant No.2009CB623304) and the National Natural Science Foundation of China (Grant No. 51002174).

References

1. G. I. Meijer, *Science*, **319**, 1625 (2008).
2. R. Waser and M. Aono, *Nature Mater.*, **6**, 833 (2007).
3. M. J. Lee, Y. Park, D. S. Suh, E. H. Lee, S. Seo, D. C. Kim, R. Jung, B. S. Kang, S. E. Ahn, C. B. Lee, et al., *Adv. Mater.*, **19**, 3919 (2007).
4. S. Q. Liu, N. J. Wu, and A. Ignatiev, *Appl. Phys. Lett.*, **76**, 2749 (2000).
5. S. Seo, M. J. Lee, D. H. Seo, S. K. Choi, D. S. Suh, Y. S. Joung, I. K. Yoo, I. S. Byun, I. R. Hwang, S. H. Kim, et al., *Appl. Phys. Lett.*, **86**, 093509 (2005).
6. B. J. Choi, D. S. Jeong, S. K. Kim, C. Rohde, S. Choi, J. H. Oh, H. J. Kim, C. S. Hwang, K. Szot, R. Waser, et al., *J. Appl. Phys.*, **98**, 033715 (2005).
7. W. Y. Chang, Y. C. Lai, T. B. Wu, S. F. Wang, F. Chen, and M. J. Tsai, *Appl. Phys. Lett.*, **92**, 022110 (2008).
8. X. Wu, P. Zhou, J. Li, L. Y. Chen, Hblyy Lin, and T. A. Tang, *Appl. Phys. Lett.*, **90**, 183507 (2007).
9. S. C. Chae, J. S. Lee, S. Kim, S. B. Lee, S. H. Chang, C. Liu, B. Kahng, H. Shin, D. W. Kim, C. U. Jung, et al., *Adv. Mater.*, **20**, 1154 (2008).
10. K. Oka, T. Yanagida, K. Nagashima, T. Kawai, J. S. Kim, and B. H. Park J. Am. Chem. Soc., **132**, 6634 (2010)
11. E. D. Herderick, K. M. Reddy, R. N. Sample, T. I. Draskovic, and N. P. Padture, *Appl. Phys. Lett.*, **95**, 203305 (2009).
12. K. Nagashima, T. Yanagida, K. Oka, M. Taniguchi, T. Kawai, J. S. Kim, and B. H. Park, *Nano Lett.*, **10**, 1359 (2010).
13. J. I. Sohn, S. S. Choi, S. M. Morris, J. S. Bendall, H. J. Coles, W.-K. Hong, G. Jo, T. Lee, and M. E. Welland, *Nano Lett.*, **10**, 4316 (2010).
14. W. Y. Chang, C. A. Lin, J. H. He, and T. B. Wu, *Appl. Phys. Lett.*, **96**, 242109 (2010).
15. D. B. Strukov, G. S. Snider, D. R. Stewart, and R. S. Williams, *Nature (London)*, **453**, 80 (2008).
16. L. W. Feng, C. Y. Chang, Y. F. Chang, T. C. Chang, S. Y. Wang, S. C. Chen, C. C. Lin, and P. W. Chiang, *Appl. Phys. Lett.*, **96**, 052111 (2010).
17. M. J. Lee, S. Seo, D. C. Kim, S. E. Ahn, D. H. Seo, I. K. Yoo, I. G. Baek, D. S. Kim, I. S. Byun, S. H. Kim, et al., *Adv. Mater.*, **19**, 73 (2007).
18. W. Y. Park, G. H. Kim, J. Y. Seok, K. M. Kim, S. J. Song, M. H. Lee, and C. S. Hwang, *Nanotechnology*, **21**, 195201 (2010).
19. B. Liu and E. S. Aydil, *J. Am. Chem. Soc.*, **131**, 3985 (2009).
20. N. Fuke, A. Fukui, A. Islam, R. Komiya, R. Yamanaka, H. Harima, and L. Han, *Sol. Energy Mater. Sol. Cells*, **93**, 720 (2009).
21. Y. C. Shin, J. Song, K. M. Kim, B. J. Choi, S. Choi, H. J. Lee, G. H. Kim, T. Eom, and C. S. Hwang, *Appl. Phys. Lett.*, **92**, 162904 (2008).
22. G. H. Kim, K. M. Kim, J. Y. Seok, H. J. Lee, D. Y. Cho, J. H. Han, and C. S. Hwang, *Nanotechnology*, **21**, 385202 (2010).
23. S. I. Kim, J. H. Lee, Y. W. Chang, S. S. Hwang, and K. H. Yoo, *Appl. Phys. Lett.*, **93**, 033503 (2008).
24. A. Sawa, *Mater. Today*, **11**, 28 (2008).
25. J. J. Yang, M. D. Pickett, X. M. Li, D. A. A. Ohlberg, D. R. Stewart, and R. S. Williams, *Nat. Nanotechnol.*, **3**, 429 (2008).
26. D. H. Kwon, K. M. Kim, J. H. Jang, J. M. Jeon, M. H. Lee, G. H. Kim, X. S. Li, G. S. Park, B. Lee, S. Han, et al., *Nat. Nanotechnol.*, **5**, 148 (2010).
27. R. J. Soukup, *J. Appl. Phys.*, **46**, 463 (1975).
28. J. J. Yang, F. Miao, M. D. Pickett, D. A. A. Ohlberg, D. R. Stewart, C. N. Lau, and R. S. Williams, *Nanotechnology*, **20**, 215201 (2009).
29. K. M. Kim, B. J. Choi, Y. C. Shin, S. Choi, and C. S. Hwang, *Appl. Phys. Lett.*, **91**, 012907 (2007).
30. R. Jung, M. J. Lee, S. Seo, D. C. Kim, G. S. Park, K. Kim, S. Ahn, Y. Park, I. K. Yoo, J. S. Kim, et al., *Appl. Phys. Lett.*, **91**, 022112(2007)